

UNCLASSIFIED



NAVAL AIR WARFARE CENTER AIRCRAFT DIVISION
PATUXENT RIVER, MARYLAND



TECHNICAL REPORT

REPORT NO: NAWCADPAX/TR-2005/38

AN INVESTIGATION OF SPALLING BEHAVIOR OF HIGH VELOCITY OXYGEN FUEL (HVOF) COATINGS ON THE 4340 STEEL AND HYTUF

by

**Dr. Eui W. Lee
William E. Frazier
Michael Leap
Bob Taylor
Henry Sanders**

23 February 2005

Approved for public release; distribution is unlimited.

UNCLASSIFIED

DEPARTMENT OF THE NAVY
NAVAL AIR WARFARE CENTER AIRCRAFT DIVISION
PATUXENT RIVER, MARYLAND

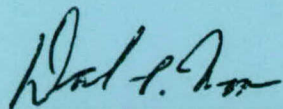
NAWCADPAX/TR-2005/38
23 February 2005

AN INVESTIGATION OF SPALLING BEHAVIOR OF HIGH VELOCITY OXYGEN FUEL
(HVOF) COATINGS ON THE 4340 STEEL AND HYTUF

by

Dr. Eui W. Lee
William E. Frazier
Michael Leap
Bob Taylor
Henry Sanders

RELEASED BY:



23 Feb 2005

DALE MOORE / AIR-4.3.4 / DATE
Head, Aerospace Materials Division
Naval Air Warfare Center Aircraft Division

REPORT DOCUMENTATION PAGE			Form Approved OMB No. 0704-0188		
Public reporting burden for this collection of information is estimated to average 1 hour per response, including the time for reviewing instructions, searching existing data sources, gathering and maintaining the data needed, and completing and reviewing this collection of information. Send comments regarding this burden estimate or any other aspect of this collection of information, including suggestions for reducing this burden, to Department of Defense, Washington Headquarters Services, Directorate for Information Operations and Reports (0704-0188), 1215 Jefferson Davis Highway, Suite 1204, Arlington, VA 22202-4302. Respondents should be aware that notwithstanding any other provision of law, no person shall be subject to any penalty for failing to comply with a collection of information if it does not display a currently valid OMB control number. PLEASE DO NOT RETURN YOUR FORM TO THE ABOVE ADDRESS.					
1. REPORT DATE 23 February 2005		2. REPORT TYPE Technical Report		3. DATES COVERED	
4. TITLE AND SUBTITLE An Investigation of Spalling Behavior of High Velocity Oxygen Fuel (HVOF) Coatings on the 4340 Steel and HyTuf		5a. CONTRACT NUMBER			
		5b. GRANT NUMBER			
		5c. PROGRAM ELEMENT NUMBER			
6. AUTHOR(S) Dr. Eui W. Lee Michael Leap Henry Sanders William E. Frazier Bob Taylor		5d. PROJECT NUMBER			
		5e. TASK NUMBER			
		5f. WORK UNIT NUMBER			
7. PERFORMING ORGANIZATION NAME(S) AND ADDRESS(ES) Naval Air Warfare Center Aircraft Division 22347 Cedar Point Road, Unit #6 Patuxent River, Maryland 20670-1161		8. PERFORMING ORGANIZATION REPORT NUMBER NAWCADPAX/TR-2005/38			
9. SPONSORING/MONITORING AGENCY NAME(S) AND ADDRESS(ES) Naval Air Systems Command 47123 Buse Road Unit IPT Patuxent River, Maryland 20670-1547		10. SPONSOR/MONITOR'S ACRONYM(S)			
		11. SPONSOR/MONITOR'S REPORT NUMBER(S)			
12. DISTRIBUTION/AVAILABILITY STATEMENT Approved for public release; distribution is unlimited.					
13. SUPPLEMENTARY NOTES					
14. ABSTRACT The application of high velocity oxygen fuel (HVOF) coatings has gained increasing acceptance in the aerospace industry. It has the potential to replace hard chromium coatings in a number of applications. This work was focused on ascertaining the limitations of HVOF coatings applied to ultra high strength steels and components experiencing high loading stresses. A group of tubular axial fatigue specimens with 2.3 in. diameter and 5.0 in. long gage section were coated with a WC-Co composite coating (Sulzer Metco Diamalloy 2005) via the HVOF process. HVOF coating thickness was varied from ~0.006 in. to ~0.012 in. and substrate material used was 4340 steel to HyTuf. The fatigue specimens were subjected to 20 cycle test segments starting at 150 ksi or 160 ksi for stress ratios of -1 and -0.33, respectively. Stepped stress testing was continued in 10 ksi increments until coating failure was observed in the form of cracking and/or spalling. Coating failure was observed to be a function of coating thickness. As coating thickness increased, coating failure occurred at progressively lower stress levels.					
15. SUBJECT TERMS Spalling; High Velocity Oxygen Fuel (HVOF); 4340 Steel; HyTuf					
16. SECURITY CLASSIFICATION OF:			17. LIMITATION OF ABSTRACT	18. NUMBER OF PAGES	19a. NAME OF RESPONSIBLE PERSON
a. REPORT	b. ABSTRACT	c. THIS PAGE			Dr. Eui W. Lee
Unclassified	Unclassified	Unclassified	SAR	43	19b. TELEPHONE NUMBER (include area code) 301-342-8071

SUMMARY

The application of high velocity oxygen fuel (HVOF) coatings has gained increasing acceptance in the aerospace industry. It has the potential to replace hard chromium coatings in a number of applications. This work was focused on ascertaining the limitations of HVOF coatings applied to ultra high strength steels and components experiencing high loading stresses. A group of tubular axial fatigue specimens with 2.3 in. diameter and 5.0 in. long gage section were coated with a WC-Co composite coating (Sulzer Metco Diamalloy 2005) via the HVOF process. HVOF coating thickness was varied from ~0.006 in. to ~0.012 in. and substrate material used was 4340 steel to HyTuf. The fatigue specimens were subjected to 20 cycle test segments starting at 150 ksi or 160 ksi for stress ratios of -1 and -0.33, respectively. Stepped stress testing was continued in 10 ksi increments until coating failure was observed in the form of cracking and/or spalling. Coating failure was observed to be a function of coating thickness. As coating thickness increased, coating failure occurred at progressively lower stress levels.

Contents

	<u>Page No.</u>
Introduction	1
Experimental Procedure	1
Test Specimens	1
Axial Fatigue Tests	2
Experimental Results	5
Single-Stress Fatigue Tests	5
Stepped-Stress Fatigue Tests	5
Damage Accumulation and Spalling in the High Velocity Oxygen Fuel Coatings	9
Discussion of Results	11
High Velocity Oxygen Fuel Coating Failure Stress	11
Mechanism of High Velocity Oxygen Fuel Coating Failure	12
Conclusions and Recommendations	17
Appendix: Data Sheets for the Axial Fatigue Tests	19
Distribution	35

List of Figures

<u>Figure No.</u>	<u>Title</u>	<u>Page No.</u>
1.	Tubular Axial Fatigue Specimen Coated with Diamalloy 2005 2 in the Gage Section	2
2.	The axial strain in a 4.0 in. gage length is shown as a function..... 4 of applied load at four angular positions on the circumference of a tubular fatigue specimen. Evaluation of these data, Equations 1 and 2, indicate that the bending strain is less than 1% of the axial strain for applied loads in the -50 kip to 50 kip range	4
3.	The (a) load-actuator displacement and (b) load-time data are..... 5 shown for the first tension stress cycle applied to specimen HVOF 17	5
4.	The axial stress associated with visible spalling of the HVOF coating 6 is shown as a function of coating thickness for stepped-stress fatigue tests conducted at (a) $R = -1$ and (b) $R = -0.33$. The numbers in parentheses represent the number of tests for multiple tests with equivalent values of coating thickness and failure stress. All the fatigue samples were machined from 4340 steel and coated with HVOF.	6
5.	Spalling characteristics as a function of the coating thickness 7 showing HyTuf exhibits a similar behavior to that of 4340 steel at R of -1.0 (a) and -0.33 (b).	7
6.	Spatial distribution of damage in specimen HVOF 3 (0.006 in. coating),..... 9 as revealed by visual and ultrasonic inspection, after 20 load cycles at 210 ksi ($R = -0.33$). Stepped stress testing comprised fatigue loading in 20 cycle test segments and 10 ksi increments starting at 160 ksi.	9
7.	Morphology of spalling exhibited by HVOF coatings in axial fatigue..... 10 tests at $R = -1$: (a) specimen HVOF 8 (0.0055 in. coating), stepped stress test to 180 ksi and (b) specimen HVOF 4 (0.0055 in. coating), stepped stress test to 200 ksi (spalling failure near the end of the gage section) followed by testing at 210 ksi (spalling failure in the gage section).	10
8.	Uniformly spaced circumferential cracks in the HVOF coating of..... 11 HyTuf specimen after the application of 20 fatigue cycles at 180 ksi and $R = -0.33$. The image was obtained under a black light after processing the specimen with dye penetrant.	11
9.	Morphology of spalling exhibited by HVOF coatings in axial fatigue..... 14 tests at $R = -0.33$: (a) specimen HVOF 7 (0.006 in. coating), stepped stress test to 190 ksi; (b) specimen HVOF 14 (0.009 in. coating), stepped stress test to 180 ksi, and; (c) specimen HVOF 30 (0.01225 in. coating) tested at 160 ksi. Arrows in (a) indicate regions of localized delamination and circumferential cracking (i.e., incipient spalling) in the gage section.	14

ACKNOWLEDGEMENTS

Funding for this effort was provided by the Office of the Chief of Naval Operations, Environmental Readiness Division (N45) through the aircraft environmental compliance research and development program (W2210). Point of contact is Mr. Steve Hartle. Also, a partial funding for the HyTuf work was provided by the V-22 program office. The author would like to thank Randy Davis for providing training and sharing his expertise of ultrasonic inspection.

INTRODUCTION

Hard chrome plating provides high strength steel with excellent wear resistance and corrosion protection. Importantly, hard chrome coatings can be used to rebuild worn and corroded components that have been removed from service for maintenance and repair. Chrome plating is used extensively in critical navy aircraft components such as landing gear cylinders, hydraulic cylinders, axles, pins, and races.

Unfortunately, chrome plating baths contain hexavalent chromium, which is a known carcinogenic. During operation, chrome plating tanks emit a hexavalent chromium mist into the air that must be ducted away and removed by scrubbers. Also, waters generated from plating operations must be disposed of as hazardous waste. These factors have provided significant motivation to reduce the use of hard chrome coatings on Navy aircraft.

Previous research and development efforts had established that high velocity oxygen fuel (HVOF) thermal spray coatings are the leading candidates for replacement of hard chrome. The types of components onto which HVOF coatings are being qualified and the year of project initiation are: (1) Landing Gear, 1998, (2) Propeller Hubs, 1999, (3) Hydraulic Actuators, 2000, and (4) Helicopter Dynamic Components, 2001.

Under Joint Test Protocol, extensive tests (fatigue, wear, corrosion) were conducted by Hard Chrome Alternative Team. The results of HVOF coated samples were compared with those of hard chrome plated. The comparison was very favorable.¹

HVOF coated samples exhibited better wear resistance, equal or better fatigue performance, and equal corrosion resistance.

The purpose of this investigation is to evaluate the effect of HVOF coating thickness, stress ratio, and steel substrate on the spalling characteristics of tubular specimens similar in dimension to typical landing gear components.

EXPERIMENTAL PROCEDURE

TEST SPECIMENS

Tubular axial fatigue specimens were manufactured from 4340 steel and HyTuf to simulate coated landing gear components, figure 1. A listing of the test specimens prepared is presented in table 1. The fatigue specimens were rough machined with a 2.05 in. inside diameter, a 5.0 in. gage length, and threaded ends. Rough machined specimens were heat treated to RC 52-53 for 4340 steel and 180-200 ksi yield strength for the HyTuf and the outside diameter ground

¹Validation of VC/Co HVOF Thermal Spray Coatings as a Replacement for Hard Chrome Plating on Aircraft Landing Gear, Environmental Security Technology Certification Program (ESTCP). Joint Group on Pollution Prevention (JG-PP). *Joint Test Report Part I: Materials Testing*, 21 Nov 2002. U.S. Hard Chrome Alternatives Team (HCAT).

to nominal dimensions between 2.285 in. and 2.306 in. to accommodate coating thicknesses ranging from 0.006 in. to 0.012 in., respectively. The variation in these dimensions reflects the manner in which coated landing gears are reworked in that the coating thickness to wall thickness ratio increases from 0.045 to 0.095 with increases in coating thickness up to 0.012 in. (i.e., coating thickness corresponding to the maximum allowable stock removal during the serviceable lifetime of landing gear). The ground specimens were then grit blasted per AMS-S-13165 with 54 grit aluminum oxide supplied at 60 psi and a 90 deg impingement angle.

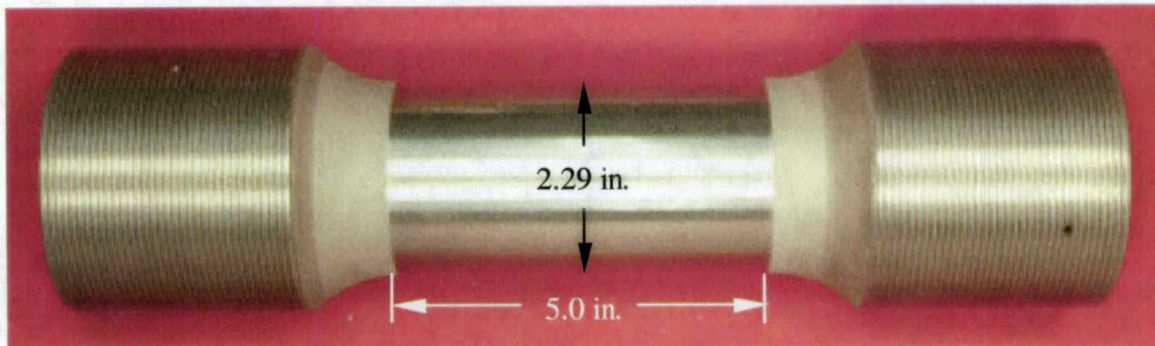


Figure 1: Tubular Axial Fatigue Specimen Coated with Diamalloy 2005 in the Gage Section

Table 1: List of Test Specimens

Specimen	Base Alloy	Nominal Coating Thickness (mils)	Standard Deviation in Coating Thickness (mils)
HVOF 1 through 8	4340 Steel	5.6	0.26
HVOF 9 through 16	4340 Steel	8.9	0.18
HVOF 17 through 30	4340 Steel	12.0	0.06
DSP No. 8	4340 Steel	11.5	N/A
HT 1 through 3	HyTuf Steel	10.8	0.43
HYT	HyTuf Steel	12.3	0.23

The fatigue specimens were coated with WC-17% Co. The coating, commercially available from Sulzer Metco under the trade name Diamalloy 2005, was applied to the fatigue specimens via the HVOF process at Hitemco in Old Bethpage, New York. An additional specimen was detonation gun coated with a DSP-1000 Detonation System at Demeton Technologies, Inc., in West Babylon, New York.

AXIAL FATIGUE TESTS

Stepped-stress axial fatigue tests were conducted on a 220 kip servohydraulic test system operating in load control. All specimens were loaded with a sinusoidal waveform at 0.5 Hz. Specimens were tested at stress ratios, R , of -1 and -0.33 in 20 cycle segments starting at maximum stress levels of 150 ksi and 160 ksi, respectively. The maximum stress for each 20

cycle segment was increased in 10 ksi increments until the coating on the specimen failed, which for the purpose of this report, is defined as the stress associated with visible cracking or spalling. For specimens tested at $R = -0.33$, the load was increased to the mean load at a rate of 2 kips/s prior to starting the fatigue test.

The stress applied to the specimen is evaluated as:

$$\sigma = \frac{4P}{\pi(d_o^2 - d_i^2)}, \quad [3]$$

where σ = applied stress, P = applied load, d_i = inside diameter of the tubular specimen, and d_o = outside diameter of the tubular specimen excluding the HVOF coating. The implicit assumption in this stress calculation is that the coating does not transmit load, which depending on the extent of damage accumulation prior to failure, could potentially overestimate the failure stress by ~5% to ~11% with increases in coating thickness from 0.006 in. to 0.012 in., respectively.

The degree of misalignment in the load train used for fatigue testing was evaluated with the general procedures outlined in ASTM E1012 by loading a tubular tensile specimen in the range between 50 kips and -50 kips. However, instead of simultaneously measuring the percent bending at discrete loads in four orthogonal positions on a strain-gaged specimen, the degree of bending was evaluated from four load-strain curves corresponding to extensometer positions located at 90 deg intervals around the circumference of the specimen. This procedure yielded the load-strain data in figure 2. A strain-based measure of specimen compliance, C_j , over a range of applied load is evaluated from the expression:

$$C_j = \frac{\sum (P_i - \bar{P})(e_i - \bar{e})}{\sum (P_i - \bar{P})^2}, \quad [1]$$

where P_i = load of the i th data point, e_i = engineering strain of the i th data point, \bar{P} = average load, \bar{e} = average engineering strain, and the subscript j refers to relative extensometer positions of 0, 90, 180, and 270 deg around the circumference of the specimen. The percentage bending, B , is estimated as:

$$B = 200 \frac{\sqrt{(C_{0^\circ} - C_{180^\circ})^2 + (C_{90^\circ} - C_{270^\circ})^2}}{\sum C_j}. \quad [2]$$

The results of this analysis indicate that the load train exhibits bending strains less than 1% of the axial strain over the -50 kip to 50 kip range.

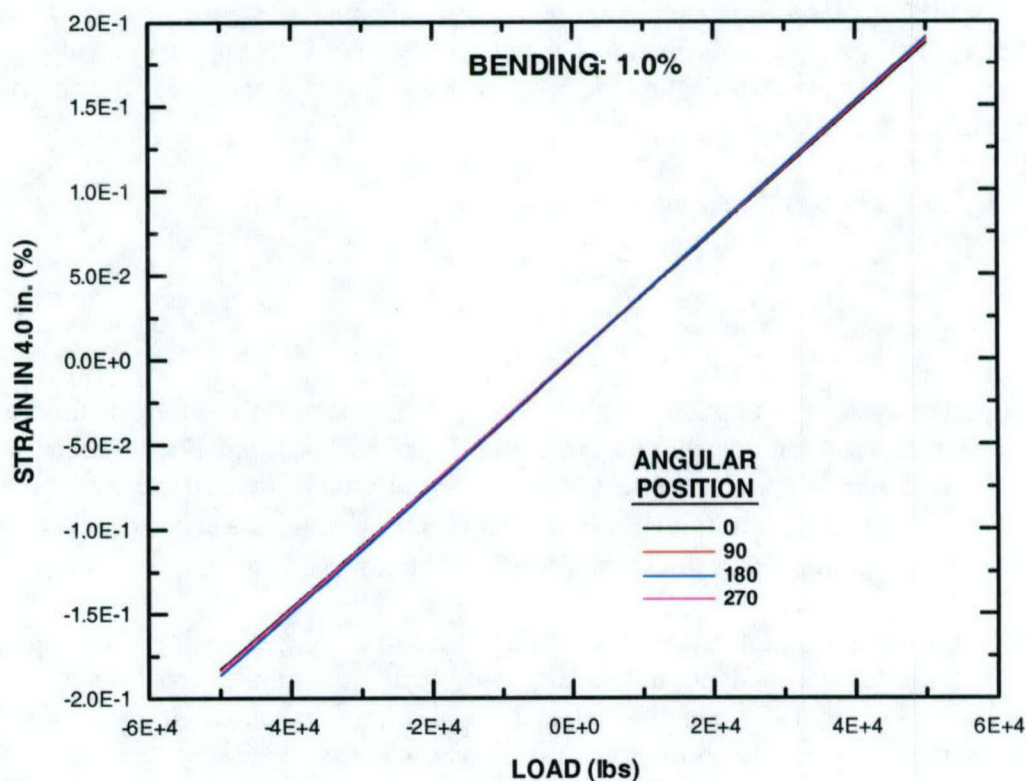


Figure 2: The axial strain in a 4.0 in. gage length is shown as a function of applied load at four angular positions on the circumference of a tubular fatigue specimen. Evaluation of these data, Equations 1 and 2, indicate that the bending strain is less than 1% of the axial strain for applied loads in the -50 kip to 50 kip range.

Damage in a thin (0.006 in.) HVOF coated specimen, HVOF 3, was monitored by visual and ultrasonic inspection. The gage section of the fatigue specimen was partitioned into 140 areas of $\sim 0.25 \text{ in.}^2$, each area corresponding to roughly 0.7% of the total surface area of the coating. The center of each area was visually and ultrasonically inspected after every 20-cycle test segment. A Krautkramer Branson USN 52 portable inspection unit with a 0.25 in. diameter piezoelectric transducer operating at 10 MHz was used for the ultrasonic inspections.

EXPERIMENTAL RESULTS

SINGLE-STRESS FATIGUE TESTS

The first test, conducted on specimen HVOF 17 (0.012 in. coating thickness), consisted of loading to 180 ksi at $R = -1$ for 20 cycles. However, the coating on the specimen exhibited catastrophic failure during the first tensile load cycle. The failure of the coating was widespread enough to momentarily affect control of the servohydraulic system, such that a failure stress of 168 ksi could be identified for spalling of the coating, figure 3. Based on this test, the starting stresses of 150 ksi and 160 ksi for subsequent tests were conducted at $R = -1$ and $R = -0.33$, respectively.

Specimen DSP 8, which was D-gun coated with a DSP-1000 Detonation System, also exhibited spalling during the first tension cycle to 160 ksi.

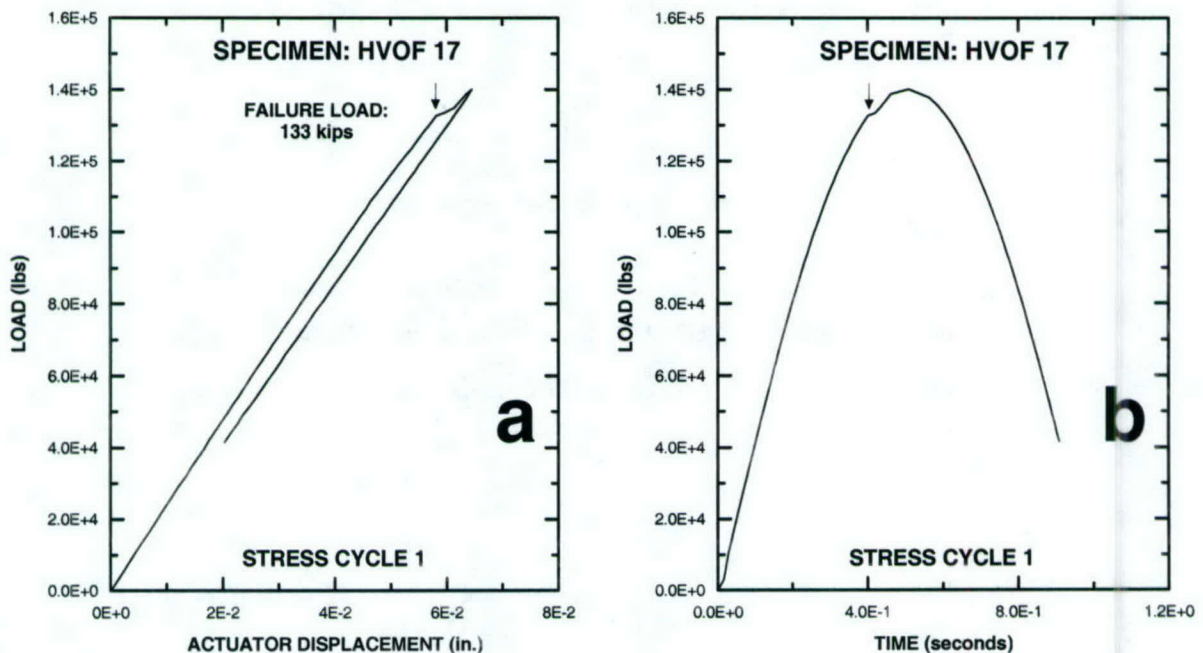


Figure 3: The (a) load-actuator displacement and (b) load-time data are shown for the first tension stress cycle applied to specimen HVOF 17.

STEPPED-STRESS FATIGUE TESTS

Data for the stepped stress tests are presented in figures 4 and 5 and table 2. Details of individual tests are tabulated in the appendix. The lower-bound axial stress for visible cracking or spalling decreases from 180 ksi to 170 ksi with increases in HVOF coating thickness from 0.0055 in. to 0.009 in. when $R = -1$. It is important to note that coating failure occurs upon initial loading for some of the specimens with 0.012 in. thick coatings.

Stepped stress tests at $R = -0.33$ exhibit an equivalent trend to the tests at $R = -1$, although the former exhibit a larger decrease in the lower-bound failure stress over the 0.006-0.009 in. range of coating thickness, figure 4.

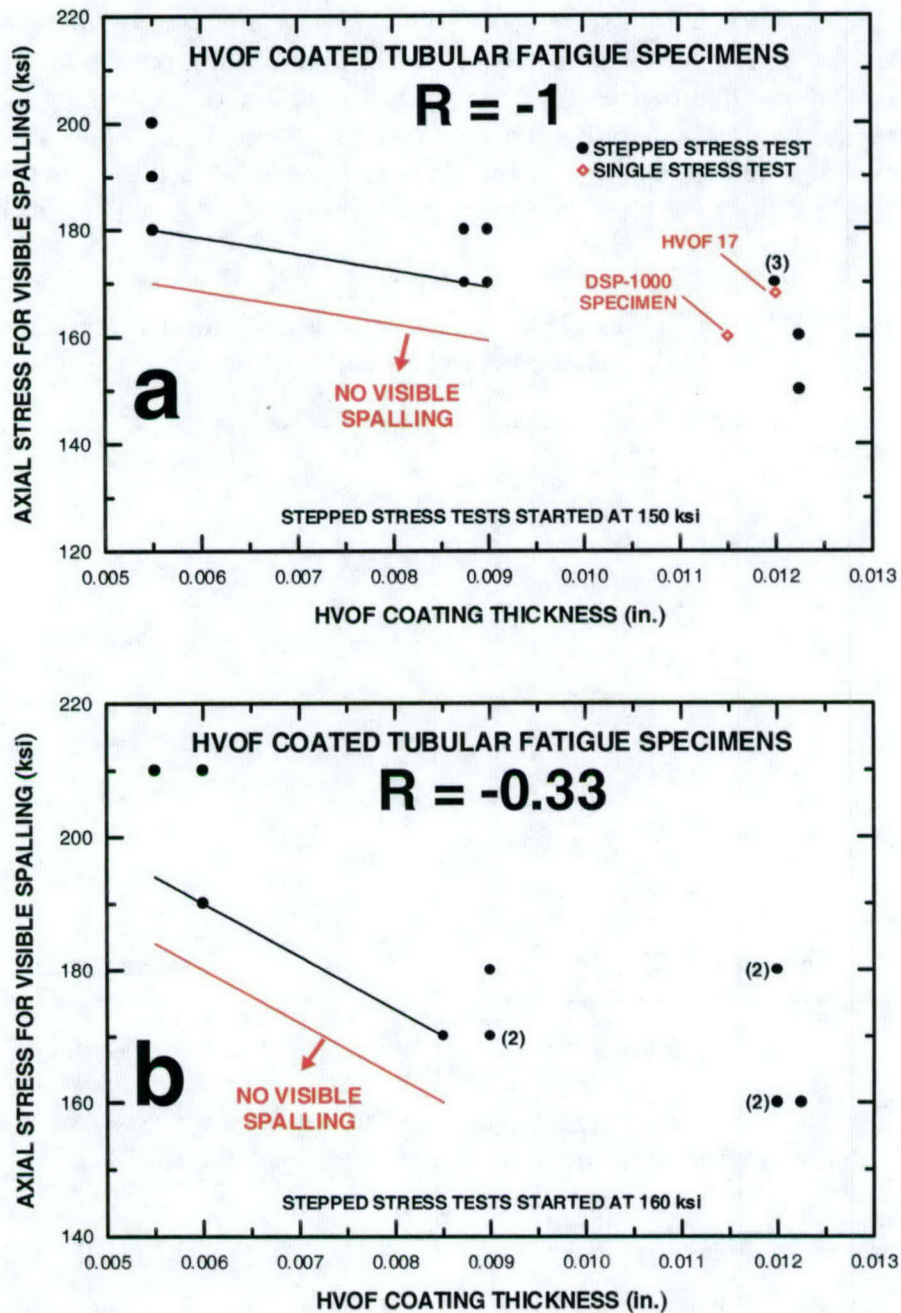


Figure 4: The axial stress associated with visible spalling of the HVOF coating is shown as a function of coating thickness for stepped-stress fatigue tests conducted at (a) $R = -1$ and (b) $R = -0.33$. The numbers in parentheses represent the number of tests for multiple tests with equivalent values of coating thickness and failure stress. All the fatigue samples were machined from 4340 steel and coated with HVOF.

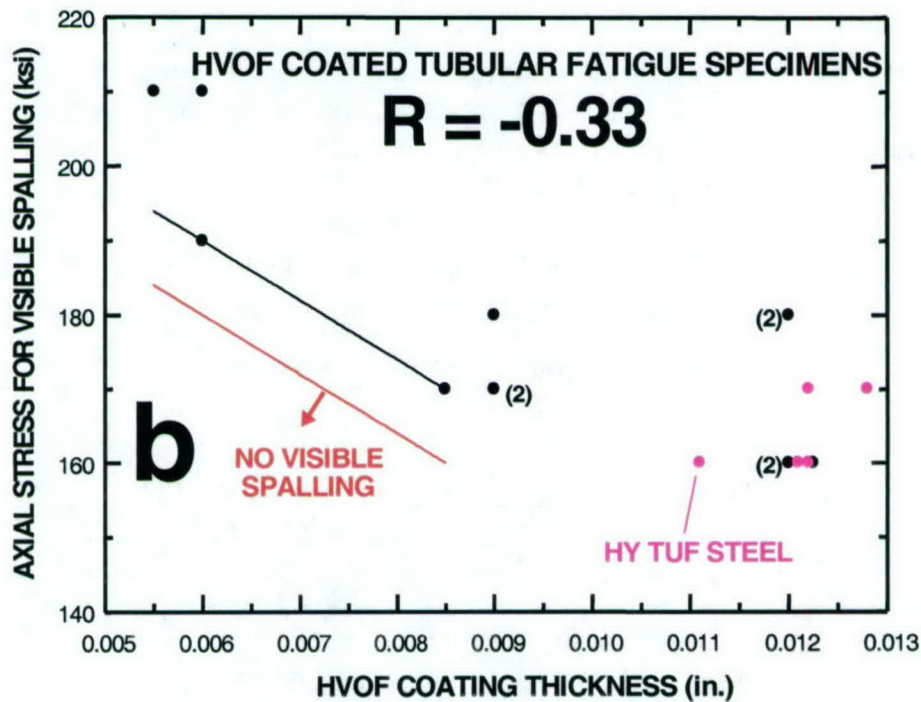
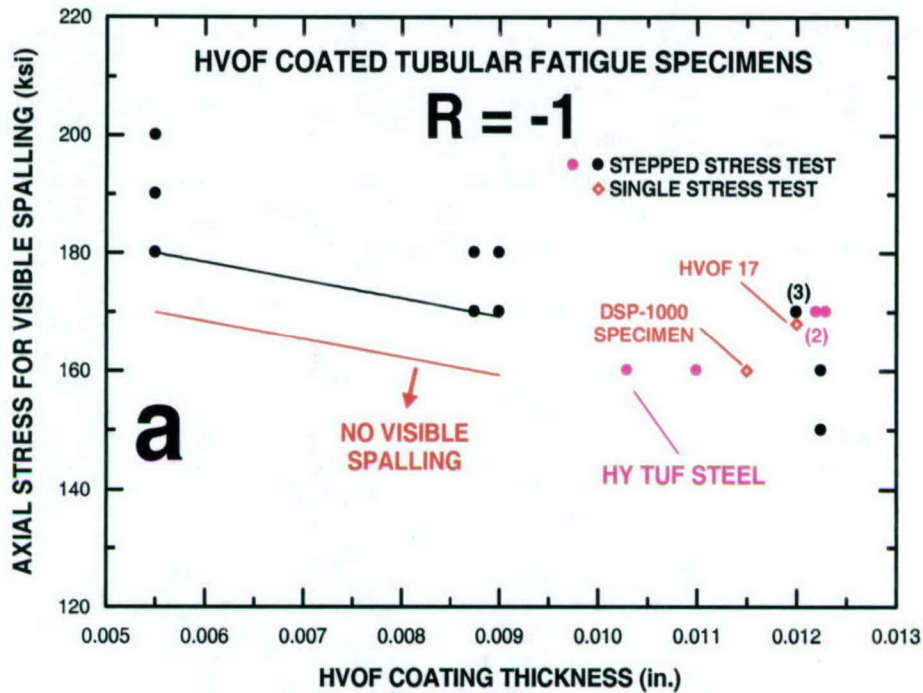


Figure 5: Spalling characteristics as a function of the coating thickness showing HyTuf exhibits a similar behavior to that of 4340 steel at R of -1.0 (a) and -0.33 (b).

Table 2: Loading Stress of HVOF Coating Specimens when Coating Failure was First Observed

	4340 Steel						HyTuf Steel	
	Coating Thickness 5.6 mil		Coating Thickness 8.9 mil		Coating Thickness 12 mil		Coating Thickness 11 - 12 mil	
Stress, ksi	R = -1	R = -0.33	R = -1	R = -0.33	R = -1	R = -0.33	R = -1	R = -0.33
150					HVOF 26			
160					HVOF 29	HVOF 20 HVOF 27 HVOF 30	HT 1 HT 3	HT 2 HYT 2 HYT 7
170			HVOF 11 HVOF 13	HVOF 10 HVOF 12 HVOF 16	HVOF 19 HVOF 21 HVOF 22		HYT 1 HYT 3 HYT 6	HYT 4 HYT 5
180	HVOF 8		HVOF 9 HVOF 15	HVOF 14	HVOF 17	HVOF 23 HVOF 24		
190	HVOF 2	HVOF 7						
200	HVOF 4							
210		HVOF 3 HVOF 5						

A statistical assessment of the mechanical property data is provided in table 3. The mean failure stress is observed to decrease with increased coating thickness. In the range of coating thickness evaluated, failure stress decreases 3.6 ksi/mil for specimens tested at R = -1 and 5.5 ksi/mil for specimens tested at R = -0.33.

Table 3: Statistical Assessment of HVOF Coating Failure Stress

	4340 Steel						HyTuf Steel	
	Coating Thickness 5.6 mil		Coating Thickness 8.9 mil		Coating Thickness 12 mil		Coating Thickness 11 - 12 mil	
Stress, ksi	R = -1	R = -0.33	R = -1	R = -0.33	R = -1	R = -0.33	R = -1	R = -0.33
X mean	190	203.3	175	172.5	166.7	168	166	164
STD	8.2	9.4	5	4.3	9.4	9.8	4.9	4.9
N	3	3	4	4	6	5	5	5
X min	180	190	170	170	150	160	160	160
X max	200	210	180	180	180	180	170	170
Lower Bound	170	180	160	160	140	150	150	150

DAMAGE ACCUMULATION AND SPALLING IN THE HIGH VELOCITY OXYGEN FUEL COATINGS

Damage of the HVOF coatings was obtained through visual and ultrasonic inspection of specimen HVOF 3 (0.006 in. coating) after every 20 cycle test segment. Visible cracking and ultrasonic indications were not observed at stresses up to 200 ksi. However, inspection revealed circumferential crack formation and limited subsurface delamination without visible spalling at the reported failure stress of 210 ksi. Figure 6 indicates the location of damage along the specimen's circumference and gauge length of the specimen as well as whether it was detected visually or through ultrasonic inspection. Unfortunately, through-section fracture during the first tensile load cycle at 220 ksi precluded any further evaluation of damage accumulation in this specimen. These data nevertheless indicate that a limited amount of damage accumulation in the form of delamination and crack formation occurs prior to spalling in the thin (0.006 in.) HVOF coatings.

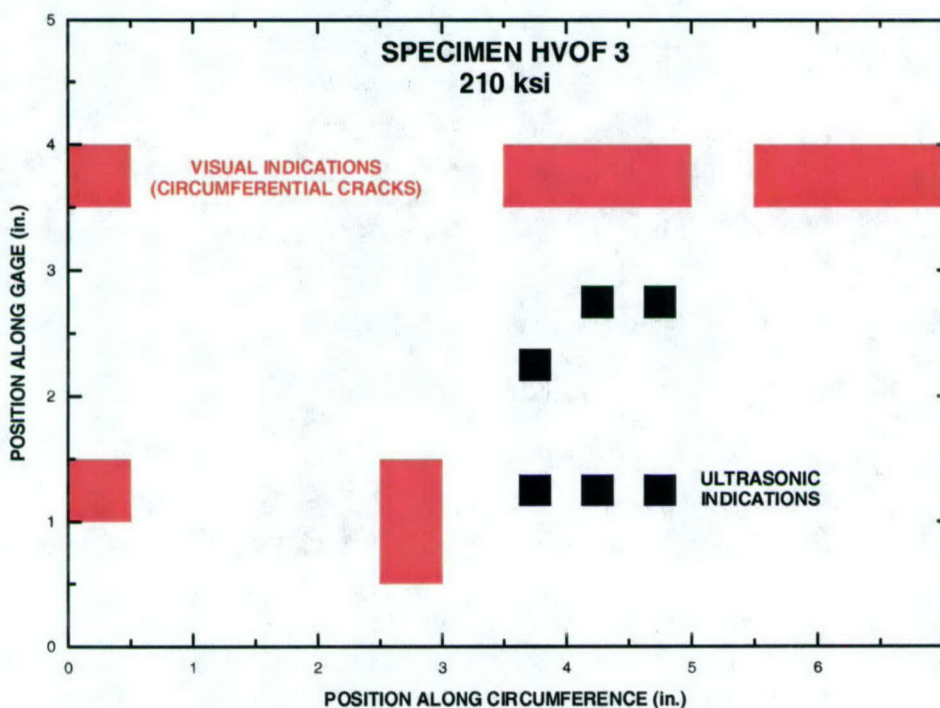


Figure 6: Spatial distribution of damage in specimen HVOF 3 (0.006 in. coating), as revealed by visual and ultrasonic inspection, after 20 load cycles at 210 ksi ($R = -0.33$).

Stepped stress testing comprised fatigue loading in 20 cycle test segments and 10 ksi increments starting at 160 ksi.

The spalling that defines coating failure in specimens tested at $R = -1$ preferentially initiates at a crack coincident with the circumferential machining blend in the steel substrate that defines the transition from the gage section to the specimen shoulder, figure 7. Cracks grow out of the circumferential crack into the specimen shoulder and arrest along a circumferential line (i.e., line of constant stress), thereby releasing sections of the coating, figure 7a. Tight

circumferential cracks also are visible to varying degrees in the gage section of the specimens, but these cracks do not initiate spalling at the failure stress. However, increases in stress above the reported failure stress initiate spalling along circumferential cracks in the gage section, figure 7b. Specimen HVOF 26 is an exception to this trend in that spalling initiated from circumferential cracks in the gage section. The only distinguishing characteristic of this specimen is that it exhibited the lowest failure stress (150 ksi) of any of the coated specimens. In contrast, the spalling that defines coating failure in specimens tested at $R = -0.33$ preferentially initiates at circumferential cracks in the gage section, figure 8. Notwithstanding specimen HVOF 5, cracking at the transition from the specimen gage to the shoulder was not apparent after testing at the reported failure stress when $R = -0.33$.

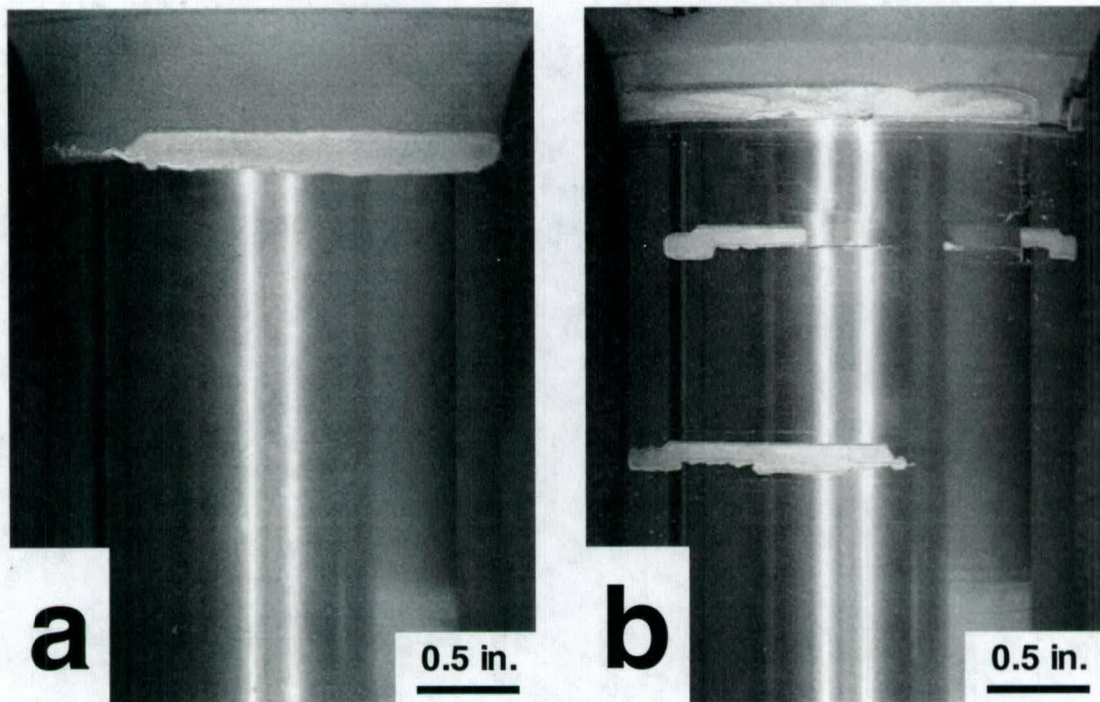


Figure 7: Morphology of spalling exhibited by HVOF coatings in axial fatigue tests at $R = -1$: (a) specimen HVOF 8 (0.0055 in. coating), stepped stress test to 180 ksi and (b) specimen HVOF 4 (0.0055 in. coating), stepped stress test to 200 ksi (spalling failure near the end of the gage section) followed by testing at 210 ksi (spalling failure in the gage section).

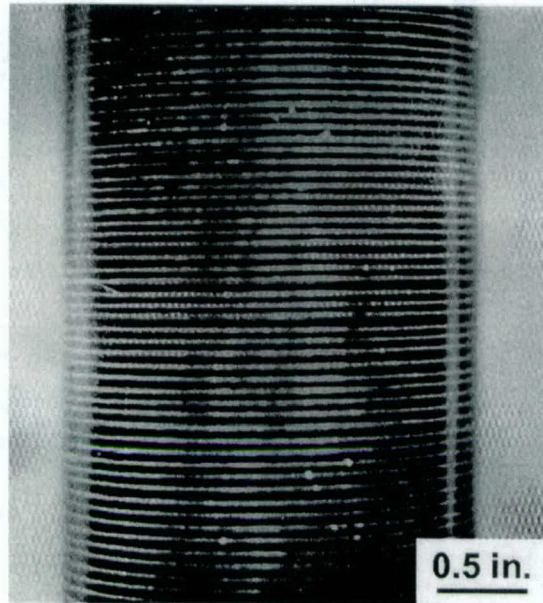


Figure 8: Uniformly spaced circumferential cracks in the HVOF coating of HyTuf specimen after the application of 20 fatigue cycles at 180 ksi and $R = -0.33$. The image was obtained under a black light after processing the specimen with dye penetrant.

DISCUSSION OF RESULTS

HIGH VELOCITY OXYGEN FUEL COATING FAILURE STRESS

Table 3 provides statistics for the mechanical tests performed. Linear regression analysis of the mean stress at which coating failure was observed results in the following equations:

For $R = -1$

$$\sigma_{\text{mean}} = -3.6t + 209 \quad [3]$$

For $R = -0.33$

$$\sigma_{\text{mean}} = -5.5t + 230 \quad [4]$$

where σ_{mean} = the mean failure stress (ksi) associated with coating retention, and t = coating thickness (mils). While linear regression provided a reasonable interpolation of the results within the range of coating thicknesses tested, the authors do not suggest that failure stress is theoretically a linear function of coating thickness.

While the mean stress at failure is of significance, it is more important to define the lower-bound stress. The lower-bound stress is the test stress at which no failure was observed. Based on a linear regression of the lower bound values obtained from the limited number of fatigue samples tested, the following expressions can be written:

$$\sigma_{\text{MAX}} = 187 - 3077t \quad (R = -1), \quad [5]$$

and:

$$\sigma_{\text{MAX}} = 228 - 8000t \quad (R = -0.33), \quad [6]$$

where σ_{MAX} = maximum stress (ksi) associated with coating retention and t = coating thickness (in.). These equations are valid for coating thickness ranging from 0.006-0.009 in.

The definition of a lower bound stress for the 0.012 in. coating thickness again is not possible since the lowest failure stress is equivalent to the starting stress (160 ksi) for the fatigue tests. Extrapolation of this linear trend beyond 0.009 in. is not possible since the lower-bound failure stress for a 0.012 in. coating may very well be less than 150 ksi (i.e., the starting stress for the fatigue tests).

It is important to note, that for engineering applications the lower-bound values may not be conservative. That is, the stress value at which 95% of the coated specimens at a confidence level of 95% will not fail may well be less than the lower bound stress.

MECHANISM OF HIGH VELOCITY OXYGEN FUEL COATING FAILURE

As indicated on the data sheets in the appendix, fatigue tests are accompanied by audible indications during the loading portion of the tensile stress cycle ($d\sigma/dt > 0$). Examination of videos taken during the tests, as well as posttest examination of the specimens, suggest that the audible indications are associated with the delamination of localized regions of the coating in conjunction with the formation of circumferential cracks on the specimen, figure 6. Visible circumferential markings immediately prior to the formation of circumferential (tensile) cracks also were observed in two specimens exhibiting regions of subsurface delamination.² Spalling of the coating, on the other hand, appears to occur after the formation of the circumferential cracks during the loading portion of a compressive stress cycle ($d\sigma/dt < 0$).

The axial fatigue data indicate that the HVOF coating is more susceptible to spalling under fully reversed bending ($R = -1$), although the increases in failure stress with stress ratio are relatively modest (0-10 ksi) and reflect a change in failure initiation site. It can be speculated that, during the loading cycle, the presence of a geometric stress due to modulus mismatch between the substrate and coating material would exceed that of the adhesion stress. This will lead to delamination during the tensile portion of a loading cycle. Finally, the cracking and spalling occur either in sequence or simultaneously. Therefore, the delamination that subsequently initiates a circumferential crack would be highly dependent on the amount of

²Refer to the data sheets in the appendix and the *.mpg files for specimens HVOF 15 and HVOF 20.

adhesion strength and modulus mismatch between the substrate and coating during the compressive portion of the loading cycle. The extent of the delamination would increase in the presence of a geometric feature such as the machining blend and/or with an increase in the maximum compressive stress. This explanation is consistent with the initiation of spalling at the gage-shoulder transition when $R = -1$ and the general absence of cracks at the gage-shoulder transition when $R = -0.33$, figures 7 and 9.³ The effect of the coating thickness on the spalling stress can be explained by the varying bendability of the coating material. It is speculated that the delamination stress may be the same for coatings of two different thicknesses. However, for the highly brittle coating material as WC-17Co, a small increase in thickness will increase the plane stress component, thus decrease the bendability. Consequently, the spalling stress for the thicker coating is lower than that of thinner coating.

It is interesting to note that the spalling stresses for the 4340 steel substrate are pretty similar to those of the HyTuf as shown in figure 5 and table 4. Considering most of the spalling occurred below yield strength of the HyTuf, it is safe to assume that delamination and spalling occur while the substrate steel is subjected to within the elastic range. Assuming that all the high strength steels exhibit a similar elastic modulus, we can reach a reasonable conclusion that the amount of strain for spalling for different high strength steels (HyTuf, 4340, Aremet 100, and 300M) would be the same. Consequently, the results obtained here can be extended to other high strength steels such as Aermet 100 and 300M.

³The two noted exceptions to the variation in failure mode with stress ratio (specimens HVOF 5 and HVOF 26) suggest that competition between different failure initiation sites may be affected by variability in the substrate and/or coating for tests conducted at each stress ratio.

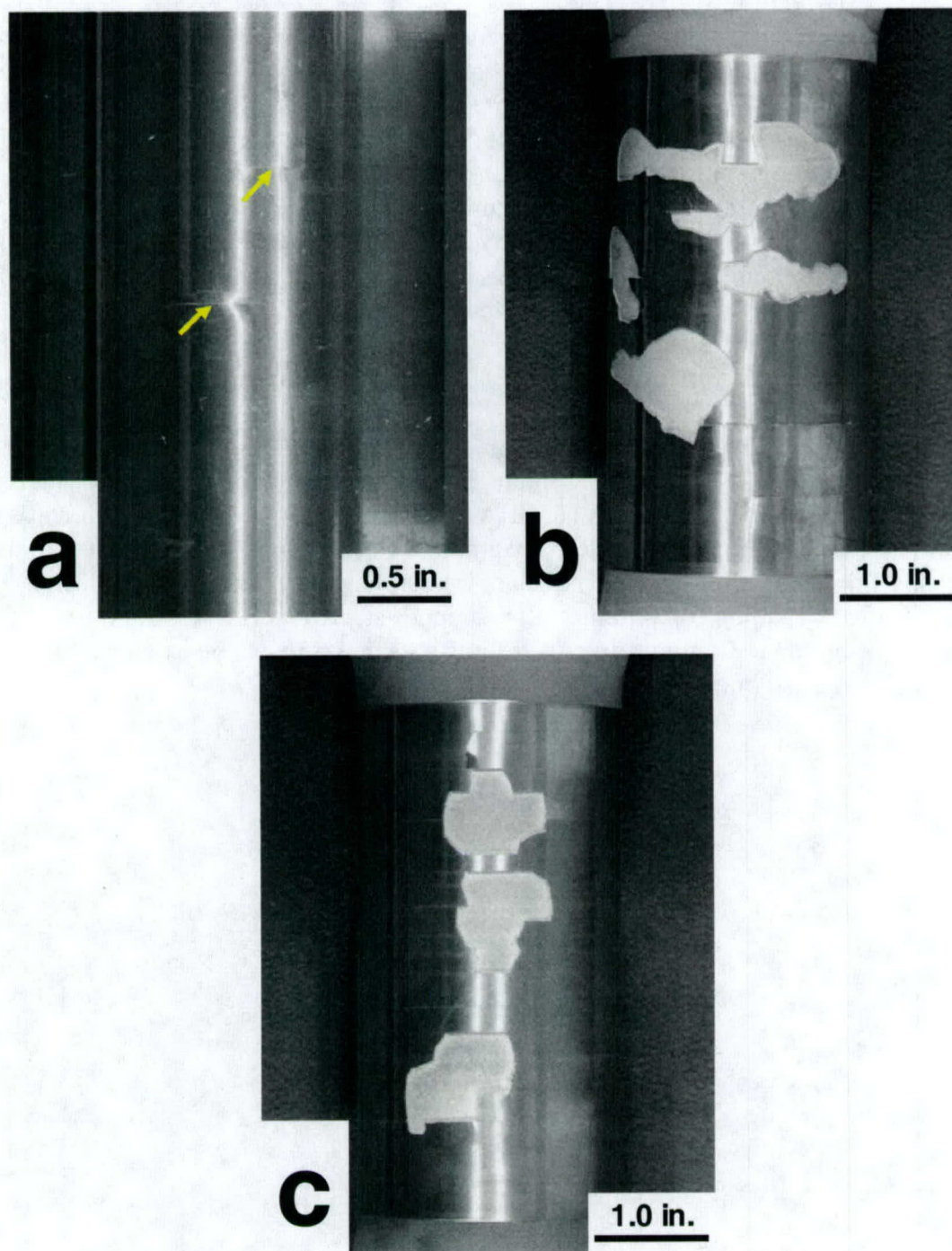


Figure 9: Morphology of spalling exhibited by HVOF coatings in axial fatigue tests at $R = -0.33$: (a) specimen HVOF 7 (0.006 in. coating), stepped stress test to 190 ksi; (b) specimen HVOF 14 (0.009 in. coating), stepped stress test to 180 ksi, and; (c) specimen HVOF 30 (0.01225 in. coating) tested at 160 ksi. Arrows in (a) indicate regions of localized delamination and circumferential cracking (i.e., incipient spalling) in the gage section.

Table 4: Summary for HyTuf Axial Test Data

SPECIMEN	HVOF COATING THICKNESS (in.)	RATIO OF COATING THICKNESS TO SUBSTRATE THICKNESS	STRESS RATIO, R	COATING FAILURE STRESS (ksi)	FAILURE MECHANISM AT THE FAILURE STRESS
HT1	0.010	0.087	-1	160	CIR. CRACKING → SPALLING
HT3	0.011	0.093	-1	160	CIRCUMFERENTIAL CRACKING
HYT1	0.012	0.104	-1	170	CIR. CRACKING → SPALLING
HYT3	0.012	0.104	-1	170	CIRCUMFERENTIAL CRACKING
HYT6	0.012	0.106	-1	170	CIRCUMFERENTIAL CRACKING
HT2	0.011	0.095	-0.33	160	CIR. CRACKING → SPALLING
HYT2	0.012	0.104	-0.33	160	CIRCUMFERENTIAL CRACKING
HYT4	0.013	0.110	-0.33	170	CIR. CRACKING → SPALLING
HYT5	0.012	0.104	-0.33	170	CIRCUMFERENTIAL CRACKING
HYT7	0.012	0.103	-0.33	160	CIRCUMFERENTIAL CRACKING

Based on these observations, a general mechanism of coating failure is proposed:

Localized regions of subsurface delamination results from the fact that elastic mismatch strain between the substrate and coating during the tensile portion of the loading cycle exceeds that of the adhesion (primary factor affecting delamination).

Circumferential cracks, figure 8, initiate from localized regions of subsurface delamination in the HVOF coating during the loading portion of tensile stress cycles. The circumferential cracks were originated because the HVOF coatings were applied circumferentially. Delamination and cracking may occur in sequence or at the same time depending on the coating thickness during the same loading cycle or during different loading cycles, figure 6. It is believed that the delamination and cracking occur in sequence for thin coating and at the same time for thick coating.

Spalling initiates at the circumferential cracks since the brittle and cracked coating cannot accommodate the compressive stress during the loading cycle.

THIS PAGE INTENTIONALLY LEFT BLANK

CONCLUSIONS AND RECOMMENDATIONS

Thinner coatings exhibit a higher failure stress than the thicker coatings. This is true for specimens tested at both stress ratios ($R = -1.0$ and -0.33).

The failure stress of specimens tested at a stress ratio of -0.33 are slightly higher (0-10 ksi) than the failure stress of specimens tested at a stress ratio of -1.0 .

The mechanism of coating failure is independent of the stress ratio employed. Failure occurs by a combination of subsurface delamination, circumferential crack initiation and propagation, and spalling from the circumferential cracks.

Although the spalling tests were conducted on the two high strength steels (4340 and HyTuf), the results are believed to be applicable to other types of high strength steels such as Aermet 100 and 300M.

The lower-bound stress represents the stress at which no coating failure was observed. No application of HVOF coatings on high strength steel is recommended when stress levels exceed the lower-bound stress. The application of HVOF coatings on high strength steels requires careful consideration of the test data provided. The further development of statistically significant design allowables and the application of an appropriate safety factor are recommended.

THIS PAGE INTENTIONALLY LEFT BLANK

APPENDIX
DATA SHEETS FOR THE AXIAL FATIGUE TESTS

4340 steel

HVOF 2, 3, 4, 5, 6, 7, 8, 9, 10, 11, 12, 13, 14, 15, 16, 17, 18, 19, 20,
21, 22, 23, 24, 26, 27, 29, 30, DSP No. 8

HyTuf

HT 1, 2, 3

HYT 1, 2, 3, 4, 5, 6, 7

SPECIMEN

HVOF 2

OUTSIDE DIAMETER (in.): 2.285
 EFFECTIVE OUTSIDE DIAMETER (in.): 2.274
 INSIDE DIAMETER (in.): 2.04
 CROSS-SECTIONAL AREA (in²): 0.7928
 (WITHOUT COATING)

NOMINAL COATING THICKNESS (in.): 0.0055

MAXIMUM STRESS (ksi)	STRESS RATIO, R	MAXIMUM LOAD (kips)	MINIMUM LOAD (kips)	STRESS CYCLES	COMMENTS
150	-1	118.9	-118.9	20	SPECIMEN SURVIVED.
160	-1	126.9	-126.9	20	SPECIMEN SURVIVED - SEVERAL AUDIBLE INDICATIONS DURING TEST.
170	-1	134.8	-134.8	20	SPECIMEN SURVIVED - SEVERAL AUDIBLE INDICATIONS STARTING FROM CYCLE 1.
180	-1	142.7	-142.7	20	SPECIMEN SURVIVED - SEVERAL AUDIBLE INDICATIONS STARTING FROM CYCLE 1.
190	-1	150.6	-150.6	<3	VISIBLE SPALLING FROM GAGE SECTION INTO SHOULDER ALONG CIRCUMFERENTIAL LINE SEPARATING GAGE AND SHOULDER.

SPECIMEN

HVOF 3

OUTSIDE DIAMETER (in.): 2.286
 EFFECTIVE OUTSIDE DIAMETER (in.): 2.274
 INSIDE DIAMETER (in.): 2.043
 CROSS-SECTIONAL AREA (in²): 0.7832
 (WITHOUT COATING)

NOMINAL COATING THICKNESS (in.): 0.006

MAXIMUM STRESS (ksi)	STRESS RATIO, R	MAXIMUM LOAD (kips)	MINIMUM LOAD (kips)	STRESS CYCLES	COMMENTS
160	-0.33	125.3	-41.8	20	AUDIBLE INDICATIONS THROUGHOUT TEST.
170	-0.33	133.1	-44.4	20	AUDIBLE INDICATIONS THROUGHOUT TEST.
180	-0.33	141	-47	20	AUDIBLE INDICATIONS THROUGHOUT TEST.
190	-0.33	148.8	-49.6	20	AUDIBLE INDICATIONS THROUGHOUT TEST.
200	-0.33	156.6	-52.2	20	AUDIBLE INDICATIONS THROUGHOUT TEST.
210	-0.33	164.5	-54.8	20	AUDIBLE INDICATIONS THROUGHOUT TEST. CIRCUMFERENTIAL CRACKS FORMED AT "STRAIN LINES".
220	-0.33	172.3	-57.4	1	SPECIMEN FAILED
LOADED AT 2 kips TO THE MEAN LOAD.					

SPECIMEN

HVOF 4

OUTSIDE DIAMETER (in.): 2.285
 EFFECTIVE OUTSIDE DIAMETER (in.): 2.274
 INSIDE DIAMETER (in.): 2.044
 CROSS-SECTIONAL AREA (in²): 0.78
 (WITHOUT COATING)

NOMINAL COATING THICKNESS (in.): 0.0055

MAXIMUM STRESS (ksi)	STRESS RATIO, R	MAXIMUM LOAD (kips)	MINIMUM LOAD (kips)	STRESS CYCLES	COMMENTS
150	-1	117	-117	20	AUDIBLE INDICATIONS DURING CYCLES 1-3.
160	-1	124.8	-124.8	20	AUDIBLE INDICATIONS THROUGHOUT TEST.
170	-1	132.6	-132.6	20	AUDIBLE INDICATIONS THROUGHOUT TEST.
180	-1	140.4	-140.4	20	AUDIBLE INDICATIONS THROUGHOUT TEST.
190	-1	148.2	-148.2	20	AUDIBLE INDICATIONS THROUGHOUT TEST.
200	-1	156	-156	20	VISIBLE SPALLING FROM CIRCUMFERENTIAL LINE IN GAGE SECTION TO SPECIMEN SHOULDER.
210	-1	163.8	-163.8	<20	COATING FAILURE IN GAGE SECTION (SPALLING AWAY FROM SHOULDER-GAGE INTERFACE).

SPECIMEN

HVOF 5

OUTSIDE DIAMETER (in.): 2.285
 EFFECTIVE OUTSIDE DIAMETER (in.): 2.274
 INSIDE DIAMETER (in.): 2.042
 CROSS-SECTIONAL AREA (in²): 0.7864
 (WITHOUT COATING)

NOMINAL COATING THICKNESS (in.): 0.0055

MAXIMUM STRESS (ksi)	STRESS RATIO, R	MAXIMUM LOAD (kips)	MINIMUM LOAD (kips)	STRESS CYCLES	COMMENTS
160	-0.33	125.8	-41.9	20	AUDIBLE INDICATIONS DURING CYCLES 6, 11, 14, 16, AND 17.
170	-0.33	133.7	-44.6	20	AUDIBLE INDICATIONS THROUGHOUT TEST, BUT NO VISIBLE SPALLING.
180	-0.33	141.6	-47.2	20	AUDIBLE INDICATIONS THROUGHOUT TEST, BUT NO VISIBLE SPALLING.
190	-0.33	149.4	-49.8	20	AUDIBLE INDICATIONS THROUGHOUT TEST, BUT NO VISIBLE SPALLING.
200	-0.33	157.3	-52.4	20	AUDIBLE INDICATIONS THROUGHOUT TEST, BUT NO VISIBLE SPALLING. CIRCUMFERENTIAL "STRAIN LINES" CLEARLY VISIBLE ON SPECIMEN.
210	-0.33	165.2	-55.1	20	CIRCUMFERENTIAL CRACK FORMED AT A "STRAIN LINE".
LOADED AT 2 kips/s TO THE MEAN LOAD.					

SPECIMEN

HVOF 6

OUTSIDE DIAMETER (in.): _____
 EFFECTIVE OUTSIDE DIAMETER (in.): _____
 INSIDE DIAMETER (in.): _____
 CROSS-SECTIONAL AREA (in²): _____
 (WITHOUT COATING)

NOMINAL COATING THICKNESS (in.): _____

MAXIMUM STRESS (ksi)	STRESS RATIO, R	MAXIMUM LOAD (kips)	MINIMUM LOAD (kips)	STRESS CYCLES	COMMENTS
					SPECIMEN QUARANTINED BY CUSTOMER

SPECIMEN

HVOF 7

OUTSIDE DIAMETER (in.): 2.286
 EFFECTIVE OUTSIDE DIAMETER (in.): 2.274
 INSIDE DIAMETER (in.): 2.045
 CROSS-SECTIONAL AREA (in²): 0.7768
 (WITHOUT COATING)

NOMINAL COATING THICKNESS (in.): 0.006

MAXIMUM STRESS (ksi)	STRESS RATIO, R	MAXIMUM LOAD (kips)	MINIMUM LOAD (kips)	STRESS CYCLES	COMMENTS
160	-0.33	124.3	-41.4	20	AUDIBLE INDICATIONS DURING CYCLES 1, 2, 6, 12, AND 18.
170	-0.33	132.1	-44	20	AUDIBLE INDICATIONS THROUGHOUT TEST, BUT NO VISIBLE SPALLING.
180	-0.33	139.8	-46.6	20	AUDIBLE INDICATIONS THROUGHOUT TEST, BUT NO VISIBLE SPALLING. CIRCUMFERENTIAL "STRAIN LINES" CLEARLY VISIBLE ON SPECIMEN.
190	-0.33	147.6	-49.2	20	CIRCUMFERENTIAL CRACKS FORMED AT "STRAIN LINES".
LOADED AT 2 kips/s TO THE MEAN LOAD.					

SPECIMEN HVOF 8

OUTSIDE DIAMETER (in.): 2.285

EFFECTIVE OUTSIDE DIAMETER (in.): 2.274

INSIDE DIAMETER (in.): 2.043

CROSS-SECTIONAL AREA (in²): 0.7832

(WITHOUT COATING)

NOMINAL COATING THICKNESS (in.): 0.0055

MAXIMUM STRESS (ksi)	STRESS RATIO, R	MAXIMUM LOAD (kips)	MINIMUM LOAD (kips)	STRESS CYCLES	COMMENTS
150	-1	117.5	-117.5	20	AUDIBLE INDICATIONS DURING CYCLES 1, 4, 7, AND 10. NO VISIBLE SPALLING.
160	-1	125.3	-125.3	20	AUDIBLE INDICATIONS THROUGHOUT TEST. NO VISIBLE SPALLING.
170	-1	133.1	-133.1	20	AUDIBLE INDICATIONS THROUGHOUT TEST. NO VISIBLE SPALLING.
180	-1	141	-141	11	VISIBLE SPALLING FROM GAGE SECTION INTO SHOULDER ALONG CIRCUMFERENTIAL LINE IN GAGE.

SPECIMEN HVOF 9

OUTSIDE DIAMETER (in.): 2.3

EFFECTIVE OUTSIDE DIAMETER (in.): 2.282

INSIDE DIAMETER (in.): 2.05

CROSS-SECTIONAL AREA (in²): 0.7893

(WITHOUT COATING)

NOMINAL COATING THICKNESS (in.): 0.009

MAXIMUM STRESS (ksi)	STRESS RATIO, R	MAXIMUM LOAD (kips)	MINIMUM LOAD (kips)	STRESS CYCLES	COMMENTS
150	-1	118.4	-118.4	20	SPECIMEN SURVIVED.
160	-1	126.3	-126.3	20	SPECIMEN SURVIVED.
170	-1	134.2	-134.2	20	AUDIBLE INDICATIONS DURING TEST, BUT NO VISIBLE SPALLING.
180	-1	142.1	-142.1	<5	AUDIBLE INDICATIONS AND VISIBLE SPALLING THROUGHOUT TEST. "ZIG ZAG" FRACTURE AT 1 = 24 k N MPQ FILE.

SPECIMEN HVOF 10

OUTSIDE DIAMETER (in.): 2.3

EFFECTIVE OUTSIDE DIAMETER (in.): 2.282

INSIDE DIAMETER (in.): 2.052

CROSS-SECTIONAL AREA (in²): 0.7829

(WITHOUT COATING)

NOMINAL COATING THICKNESS (in.): 0.009

MAXIMUM STRESS (ksi)	STRESS RATIO, R	MAXIMUM LOAD (kips)	MINIMUM LOAD (kips)	STRESS CYCLES	COMMENTS
160	-0.33	125.3	-41.8	20	AUDIBLE INDICATIONS THROUGHOUT TEST STARTING AT CYCLE 1. NO VISIBLE SPALLING.
170	-0.33	133.1	-44.4	<20	AUDIBLE INDICATIONS AND VISIBLE SPALLING IN GAGE SECTION THROUGHOUT TEST.
LOADED AT 2 kips/s TO THE MEAN LOAD.					

SPECIMEN

HVOF 11

OUTSIDE DIAMETER (in.): 2.3
 EFFECTIVE OUTSIDE DIAMETER (in.): 2.282
 INSIDE DIAMETER (in.): 2.052
 CROSS-SECTIONAL AREA (in²): 0.7829
 (WITHOUT COATING)

NOMINAL COATING THICKNESS (in.): 0.009

MAXIMUM STRESS (ksi)	STRESS RATIO, R	MAXIMUM LOAD (kips)	MINIMUM LOAD (kips)	STRESS CYCLES	COMMENTS
150	-1	117.4	-117.4	20	AUDIBLE INDICATIONS STARTING FROM CYCLE 1.
160	-1	125.3	-125.3	20	AUDIBLE INDICATIONS DURING CYCLES 1, 6, AND 7.
170	-1	133.1	-133.1	20	VISIBLE SPALLING FROM CIRCUMFERENTIAL LINE IN GAGE SECTION TO SPECIMEN SHOULDER.
180	-1	140.9	-140.9	20	TEST CONTINUED - COATING FAILURE IN GAGE SECTION (SPALLING AWAY FROM SHOULDER-GAGE INTERFACE)

SPECIMEN

HVOF 12

OUTSIDE DIAMETER (in.): 2.299
 EFFECTIVE OUTSIDE DIAMETER (in.): 2.282
 INSIDE DIAMETER (in.): 2.054
 CROSS-SECTIONAL AREA (in²): 0.7765
 (WITHOUT COATING)

NOMINAL COATING THICKNESS (in.): 0.0085

MAXIMUM STRESS (ksi)	STRESS RATIO, R	MAXIMUM LOAD (kips)	MINIMUM LOAD (kips)	STRESS CYCLES	COMMENTS
160	-0.33	124.2	-41.4	20	AUDIBLE INDICATIONS THROUGHOUT TEST, BUT NO VISIBLE SPALLING.
170	-0.33	132	-44	20	AUDIBLE INDICATIONS DURING CYCLES 1, 4, AND 7. VISIBLE SPALLING PAST
LOADED AT 2 kips TO THE MEAN LOAD.					

SPECIMEN

HVOF 13

OUTSIDE DIAMETER (in.): 2.2995
 EFFECTIVE OUTSIDE DIAMETER (in.): 2.282
 INSIDE DIAMETER (in.): 2.054
 CROSS-SECTIONAL AREA (in²): 0.7765
 (WITHOUT COATING)

NOMINAL COATING THICKNESS (in.): 0.00875

MAXIMUM STRESS (ksi)	STRESS RATIO, R	MAXIMUM LOAD (kips)	MINIMUM LOAD (kips)	STRESS CYCLES	COMMENTS
150	-1	116.5	-116.5	20	AUDIBLE INDICATIONS DURING CYCLES 1, 2, AND 8.
160	-1	124.2	-124.2	20	AUDIBLE INDICATION DURING CYCLE 18.
170	-1	132	-132	11	AUDIBLE INDICATIONS DURING CYCLES 1 AND 2. CRACKING AT CIRCUMFERENTIAL "STRAIN LINE" AND SPALLING DURING CYCLE 11.

SPECIMEN

HVOF 14

OUTSIDE DIAMETER (in.): 2.3
 EFFECTIVE OUTSIDE DIAMETER (in.): 2.282
 INSIDE DIAMETER (in.): 2.053
 CROSS-SECTIONAL AREA (in²): 0.7797
 (WITHOUT COATING)

NOMINAL COATING THICKNESS (in.): 0.009

MAXIMUM STRESS (ksi)	STRESS RATIO, R	MAXIMUM LOAD (kips)	MINIMUM LOAD (kips)	STRESS CYCLES	COMMENTS
160	-0.33	124.7	-41.6	20	AUDIBLE INDICATION DURING CYCLE 1.
170	-0.33	132.5	-44.2	20	AUDIBLE INDICATIONS THROUGHOUT TEST.
180	-0.33	140.3	-46.8	3	VISIBLE CIRCUMFERENTIAL CRACK FORMED AT CYCLE 1. VISIBLE SPALLING DURING CYCLE 3.
LOADED AT 2 kips/s TO THE MEAN LOAD.					

SPECIMEN

HVOF 15

OUTSIDE DIAMETER (in.): 2.2995
 EFFECTIVE OUTSIDE DIAMETER (in.): 2.282
 INSIDE DIAMETER (in.): 2.05
 CROSS-SECTIONAL AREA (in²): 0.7893
 (WITHOUT COATING)

NOMINAL COATING THICKNESS (in.): 0.00875

MAXIMUM STRESS (ksi)	STRESS RATIO, R	MAXIMUM LOAD (kips)	MINIMUM LOAD (kips)	STRESS CYCLES	COMMENTS
150	-1	118.4	-118.4	20	AUDIBLE INDICATION DURING CYCLE 3.
160	-1	126.3	-126.3	20	
170	-1	134.2	-134.2	20	AUDIBLE INDICATIONS DURING CYCLES 1, 4, AND 6.
180	-1	142.1	-142.1	2	VISIBLE SPALLING DURING CYCLE 2. "ZIG-ZAG" FRACTURE NEAR GAGE-SHOULDER INTERFACE AT 1.8 IN MPG FILE.

SPECIMEN

HVOF 16

OUTSIDE DIAMETER (in.): 2.3
 EFFECTIVE OUTSIDE DIAMETER (in.): 2.282
 INSIDE DIAMETER (in.): 2.052
 CROSS-SECTIONAL AREA (in²): 0.7829
 (WITHOUT COATING)

NOMINAL COATING THICKNESS (in.): 0.009

MAXIMUM STRESS (ksi)	STRESS RATIO, R	MAXIMUM LOAD (kips)	MINIMUM LOAD (kips)	STRESS CYCLES	COMMENTS
160	-0.33	125.3	-41.8	20	AUDIBLE INDICATION DURING CYCLE 1.
170	-0.33	133.1	-44.4	2	VISIBLE CIRCUMFERENTIAL CRACK FORMED DURING CYCLE 1. VISIBLE SPALLING DURING CYCLE 2.
LOADED AT 2 kips/s TO THE MEAN LOAD.					

SPECIMEN HVOF 17

OUTSIDE DIAMETER (in.): 2.306
 EFFECTIVE OUTSIDE DIAMETER (in.): 2.282
 INSIDE DIAMETER (in.): 2.05
 CROSS-SECTIONAL AREA (in²): 0.7893
 (WITHOUT COATING)

NOMINAL COATING THICKNESS (in.): 0.012

MAXIMUM STRESS (ksi)	STRESS RATIO, R	MAXIMUM LOAD (kips)	MINIMUM LOAD (kips)	STRESS CYCLES	COMMENTS
177.5	-1	140.13	-140.13	1	COATING FAILURE AT 166 ksi

SPECIMEN HVOF 18

OUTSIDE DIAMETER (in.):
 EFFECTIVE OUTSIDE DIAMETER (in.):
 INSIDE DIAMETER (in.):
 CROSS-SECTIONAL AREA (in²):
 (WITHOUT COATING)

NOMINAL COATING THICKNESS (in.):

MAXIMUM STRESS (ksi)	STRESS RATIO, R	MAXIMUM LOAD (kips)	MINIMUM LOAD (kips)	STRESS CYCLES	COMMENTS
					SPECIMEN QUARANTINED BY CUSTOMER

SPECIMEN HVOF 19

OUTSIDE DIAMETER (in.): 2.306
 EFFECTIVE OUTSIDE DIAMETER (in.): 2.282
 INSIDE DIAMETER (in.): 2.053
 CROSS-SECTIONAL AREA (in²): 0.7797
 (WITHOUT COATING)

NOMINAL COATING THICKNESS (in.): 0.012

MAXIMUM STRESS (ksi)	STRESS RATIO, R	MAXIMUM LOAD (kips)	MINIMUM LOAD (kips)	STRESS CYCLES	COMMENTS
150	-1	117	-117	20	AUDIBLE INDICATIONS DURING CYCLES 4 AND 5.
160	-1	124.7	-124.7	20	AUDIBLE INDICATIONS DURING CYCLES 7, 8, AND 10.
170	-1	132.5	-132.5	1	CATASTROPHIC COATING FAILURE DURING CYCLE 1.

SPECIMEN HVOF 20

OUTSIDE DIAMETER (in.): 2.306
 EFFECTIVE OUTSIDE DIAMETER (in.): 2.282
 INSIDE DIAMETER (in.): 2.053
 CROSS-SECTIONAL AREA (in²): 0.7797
 (WITHOUT COATING)

NOMINAL COATING THICKNESS (in.): 0.012

MAXIMUM STRESS (ksi)	STRESS RATIO, R	MAXIMUM LOAD (kips)	MINIMUM LOAD (kips)	STRESS CYCLES	COMMENTS
160	-0.33	124.7	-41.6	<20	VISIBLE SPALLING FROM CIRCUMFERENTIAL LINE IN GAGE SECTION TO SPECIMEN SHOULDER
LOADED AT 2 kips/s TO THE MEAN LOAD.					"ZIG-ZAG" FRACTURE APPEARANCE AT 1 = 47 # IN MPG FILE

SPECIMEN HVOF 21

OUTSIDE DIAMETER (in.): 2.306
 EFFECTIVE OUTSIDE DIAMETER (in.): 2.282
 INSIDE DIAMETER (in.): 2.054
 CROSS-SECTIONAL AREA (in²): 0.77645
 (WITHOUT COATING)

NOMINAL COATING THICKNESS (in.): 0.012

MAXIMUM STRESS (ksi)	STRESS RATIO, R	MAXIMUM LOAD (kips)	MINIMUM LOAD (kips)	STRESS CYCLES	COMMENTS
150	-1	116.5	-116.5	20	AUDIBLE INDICATIONS DURING CYCLES 1 AND 2
160	-1	124.2	-124.2	20	AUDIBLE INDICATIONS DURING CYCLES 4 AND 17
170	-1	132	-132	1	CATASTROPHIC COATING FAILURE DURING CYCLE 1

SPECIMEN HVOF 22

OUTSIDE DIAMETER (in.): 2.306
 EFFECTIVE OUTSIDE DIAMETER (in.): 2.282
 INSIDE DIAMETER (in.): 2.056
 CROSS-SECTIONAL AREA (in²): 0.77
 (WITHOUT COATING)

NOMINAL COATING THICKNESS (in.): 0.012

MAXIMUM STRESS (ksi)	STRESS RATIO, R	MAXIMUM LOAD (kips)	MINIMUM LOAD (kips)	STRESS CYCLES	COMMENTS
150	-1	115.5	-115.5	20	AUDIBLE INDICATIONS DURING CYCLE 1
160	-1	123.2	-123.3	20	SEVERAL MINOR AUDIBLE INDICATIONS DURING TEST
170	-1	130.9	-130.9	4	VISIBLE SPALLING FROM CIRCUMFERENTIAL LINE IN GAGE SECTION TO SPECIMEN SHOULDER
					GOOD MPG FILE TO OBSERVE DEBONDING PRIOR TO SPALLING

SPECIMEN

HVOF 23

OUTSIDE DIAMETER (in.): 2.306
 EFFECTIVE OUTSIDE DIAMETER (in.): 2.282
 INSIDE DIAMETER (in.): 2.053
 CROSS-SECTIONAL AREA (in²): 0.7797
 (WITHOUT COATING)

NOMINAL COATING THICKNESS (in.): 0.012

MAXIMUM STRESS (ksi)	STRESS RATIO, R	MAXIMUM LOAD (kips)	MINIMUM LOAD (kips)	STRESS CYCLES	COMMENTS
160	-0.33	124.8	-41.6	20	AUDIBLE INDICATIONS DURING CYCLE 1.
170	-0.33	132.5	-44.2	20	AUDIBLE INDICATIONS DURING CYCLES 8, 11, AND PAST 15. CIRCUMFERENTIAL "STRAIN LINES" VISIBLE DURING SPECIMEN LOADING.
180	-0.33	140.34	-46.8	1	VISIBLE SPALLING FROM CIRCUMFERENTIAL LINE IN GAGE SECTION TO SPECIMEN SHOULDER.
LOADED AT 2 kips/s TO THE MEAN LOAD.					

SPECIMEN

HVOF 24

OUTSIDE DIAMETER (in.): 2.306
 EFFECTIVE OUTSIDE DIAMETER (in.): 2.282
 INSIDE DIAMETER (in.): 2.053
 CROSS-SECTIONAL AREA (in²): 0.7797
 (WITHOUT COATING)

NOMINAL COATING THICKNESS (in.): 0.012

MAXIMUM STRESS (ksi)	STRESS RATIO, R	MAXIMUM LOAD (kips)	MINIMUM LOAD (kips)	STRESS CYCLES	COMMENTS
160	-0.33	124.7	-41.6	20	AUDIBLE INDICATION DURING CYCLE 1.
170	-0.33	132.54	-44.2	20	
180	-0.33	140.34	-46.78	3	VISIBLE SPALLING FROM CIRCUMFERENTIAL LINE IN GAGE SECTION TO SPECIMEN SHOULDER.
LOADED AT 2 kips/s TO THE MEAN LOAD.					

SPECIMEN

HVOF 26

OUTSIDE DIAMETER (in.): 2.3065
 EFFECTIVE OUTSIDE DIAMETER (in.): 2.282
 INSIDE DIAMETER (in.): 2.052
 CROSS-SECTIONAL AREA (in²): 0.7829
 (WITHOUT COATING)

NOMINAL COATING THICKNESS (in.): 0.01225

MAXIMUM STRESS (ksi)	STRESS RATIO, R	MAXIMUM LOAD (kips)	MINIMUM LOAD (kips)	STRESS CYCLES	COMMENTS
150	-1	117.4	-117.4	19	AUDIBLE INDICATIONS THROUGHOUT TEST. VISIBLE SPALLING ALONG CIRCUMFERENTIAL "STRAIN LINE" DURING CYCLE 19.

SPECIMEN

HVOF 27

OUTSIDE DIAMETER (in.): 2.306

EFFECTIVE OUTSIDE DIAMETER (in.): 2.282

INSIDE DIAMETER (in.): 2.053

CROSS-SECTIONAL AREA (in²): 0.7797

(WITHOUT COATING)

NOMINAL COATING THICKNESS (in.): 0.012

MAXIMUM STRESS (ksi)	STRESS RATIO, R	MAXIMUM LOAD (kips)	MINIMUM LOAD (kips)	STRESS CYCLES	COMMENTS
160	-0.33	124.7	-41.6	1	VISIBLE CIRCUMFERENTIAL CRACK FORMED DURING CYCLE 1 VISIBLE SPALLING DURING CYCLE 8
LOADED AT 2 kips/s TO THE MEAN LOAD.					

SPECIMEN

HVOF 29

OUTSIDE DIAMETER (in.): 2.3065

EFFECTIVE OUTSIDE DIAMETER (in.): 2.282

INSIDE DIAMETER (in.): 2.053

CROSS-SECTIONAL AREA (in²): 0.7797

(WITHOUT COATING)

NOMINAL COATING THICKNESS (in.): 0.01225

MAXIMUM STRESS (ksi)	STRESS RATIO, R	MAXIMUM LOAD (kips)	MINIMUM LOAD (kips)	STRESS CYCLES	COMMENTS
150	-1	117	-117	20	AUDIBLE INDICATIONS DURING CYCLES 1, 4, AND 10.
160	-1	124.7	-124.7	1	VISIBLE SPALLING IN GAGE SECTION

SPECIMEN

HVOF 30

OUTSIDE DIAMETER (in.): 2.3065

EFFECTIVE OUTSIDE DIAMETER (in.): 2.282

INSIDE DIAMETER (in.): 2.052

CROSS-SECTIONAL AREA (in²): 0.7829

(WITHOUT COATING)

NOMINAL COATING THICKNESS (in.): 0.01225

MAXIMUM STRESS (ksi)	STRESS RATIO, R	MAXIMUM LOAD (kips)	MINIMUM LOAD (kips)	STRESS CYCLES	COMMENTS
160	-0.33	125.3	-41.8	1	VISIBLE CIRCUMFERENTIAL CRACKS AND SPALLING DURING CYCLE 1
LOADED AT 2 kips/s TO THE MEAN LOAD.					

SPECIMEN DSP #8OUTSIDE DIAMETER (in.): 2.266EFFECTIVE OUTSIDE DIAMETER (in.): 2.243INSIDE DIAMETER (in.): 2.055CROSS-SECTIONAL AREA (in²): 0.6346
(WITHOUT COATING)NOMINAL COATING THICKNESS (in.): 0.0115

MAXIMUM STRESS (ksi)	STRESS RATIO, R	MAXIMUM LOAD (kips)	MINIMUM LOAD (kips)	STRESS CYCLES	COMMENTS
160	-1	101.5	-101.5	20	CATASTROPHIC COATING FAILURE DURING CYCLE 1.
170	-1	107.9	-107.9	20	TEST CONTINUED TO FURTHER STUDY COATING FAILURE MODE.
SPECIMEN COATED WITH DSP-1000 DETONATION SYSTEM					

SPECIMEN: HT 1

OUTSIDE DIAMETER (in.): 2.3036
 EFFECTIVE OUTSIDE DIAMETER (in.): 2.283
 INSIDE DIAMETER (in.): 2.047
 CROSS-SECTIONAL AREA (in²): 0.8026
 (WITHOUT COATING)

NOMINAL COATING THICKNESS (in.): 0.0103

MAXIMUM STRESS (ksi)	STRESS RATIO, R	MAXIMUM LOAD (kips)	MINIMUM LOAD (kips)	STRESS CYCLES	COMMENTS
150	-1	120.4	-120.4	20	NUMEROUS AUDIBLE INDICATIONS DURING CYCLES 1 AND 2.
160	-1	128.4	-128.4	20	AUDIBLE INDICATIONS DURING CYCLES 1 AND 2 WITH SPALLING DURING CYCLE 2 AND BEYOND.

SPECIMEN: HT 2

OUTSIDE DIAMETER (in.): 2.3052
 EFFECTIVE OUTSIDE DIAMETER (in.): 2.283
 INSIDE DIAMETER (in.): 2.049
 CROSS-SECTIONAL AREA (in²): 0.7961
 (WITHOUT COATING)

NOMINAL COATING THICKNESS (in.): 0.0111

MAXIMUM STRESS (ksi)	STRESS RATIO, R	MAXIMUM LOAD (kips)	MINIMUM LOAD (kips)	STRESS CYCLES	COMMENTS
150	-0.33	119.4	-39.8	20	NUMEROUS AUDIBLE INDICATIONS DURING CYCLE 1.
160	-0.33	127.4	-42.5	20	CIRCUMFERENTIAL CRACKING FOLLOWED BY SPALLING.
LOADED AT 2 kips TO THE MEAN LOAD.					

SPECIMEN: HT 3

OUTSIDE DIAMETER (in.): 2.306
 EFFECTIVE OUTSIDE DIAMETER (in.): 2.284
 INSIDE DIAMETER (in.): 2.048
 CROSS-SECTIONAL AREA (in²): 0.8030
 (WITHOUT COATING)

NOMINAL COATING THICKNESS (in.): 0.0110

MAXIMUM STRESS (ksi)	STRESS RATIO, R	MAXIMUM LOAD (kips)	MINIMUM LOAD (kips)	STRESS CYCLES	COMMENTS
150	-1	120.4	-120.4	20	NUMEROUS AUDIBLE INDICATIONS DURING CYCLE 1 AND PERIODICALLY THROUGHOUT TEST SEGMENT.
160	-1	128.5	-128.5	20	AUDIBLE INDICATIONS THROUGHOUT TEST; CIRCUMFERENTIAL CRACK VISIBLE AT COMPLETION OF TEST SEGMENT.
170	-1	136.5	-136.5	20	CATASTROPHIC SPALLING DURING CYCLE 1.

SPECIMEN: HYT 1

OUTSIDE DIAMETER (in.): 2.2645
 EFFECTIVE OUTSIDE DIAMETER (in.): 2.240
 INSIDE DIAMETER (in.): 2.004
 CROSS-SECTIONAL AREA (in²): 0.7866
 (WITHOUT COATING)

NOMINAL COATING THICKNESS (in.): 0.0123

MAXIMUM STRESS (ksi)	STRESS RATIO, R	MAXIMUM LOAD (kips)	MINIMUM LOAD (kips)	STRESS CYCLES	COMMENTS
140	-1	110.1	-110.1	20	AUDIBLE INDICATIONS DURING CYCLES 1 AND 2.
150	-1	118.0	-118.0	20	
160	-1	125.9	-125.9	20	AUDIBLE INDICATIONS DURING CYCLES 5 AND 8 AND COATING FAILURE DURING CYCLE 10.
170	-1	133.7	-133.7	20	

SPECIMEN: HYT 2

OUTSIDE DIAMETER (in.): 2.2633
 EFFECTIVE OUTSIDE DIAMETER (in.): 2.239
 INSIDE DIAMETER (in.): 2.0045
 CROSS-SECTIONAL AREA (in²): 0.7816
 (WITHOUT COATING)

NOMINAL COATING THICKNESS (in.): 0.0122

MAXIMUM STRESS (ksi)	STRESS RATIO, R	MAXIMUM LOAD (kips)	MINIMUM LOAD (kips)	STRESS CYCLES	COMMENTS
150	-0.33	117.2	-39.1	20	NUMEROUS AUDIBLE INDICATIONS DURING CYCLE 1.
160	-0.33	125.0	-41.7	20	NUMEROUS AUDIBLE INDICATIONS DURING CYCLE 1. GAGE SECTION COVERED WITH EVENLY SPACED CRACKS AT TEST COMPLETION.
170	-0.33	132.9	-44.3	20	TEST CONTINUED: NO AUDIBLE INDICATIONS OF DELAMINATION DURING TEST SEGMENT.
180	-0.33	140.7	-46.9	20	TEST CONTINUED: NO AUDIBLE INDICATIONS OF DELAMINATION DURING TEST SEGMENT.
LOADED AT 2 kips TO THE MEAN LOAD.					

SPECIMEN: HYT 3

OUTSIDE DIAMETER (in.): 2.2643
 EFFECTIVE OUTSIDE DIAMETER (in.): 2.240
 INSIDE DIAMETER (in.): 2.005
 CROSS-SECTIONAL AREA (in²): 0.7835
 (WITHOUT COATING)

NOMINAL COATING THICKNESS (in.): 0.0122

MAXIMUM STRESS (ksi)	STRESS RATIO, R	MAXIMUM LOAD (kips)	MINIMUM LOAD (kips)	STRESS CYCLES	COMMENTS
150	-1	117.5	-117.5	20	AUDIBLE INDICATION DURING CYCLE 1.
160	-1	125.4	-125.4	20	AUDIBLE INDICATION DURING CYCLE 3.
170	-1	133.2	-133.2	20	FINE CIRCUMFERENTIAL CRACKS ALONGS GAGE LENGTH AT THE END OF THE TEST SEGMENT.
180	-1	141.0	-141.0	20	TEST CONTINUED WITH ADDITIONAL CRACK FORMATION BUT NO SPALLING.

SPECIMEN: HYT 4

OUTSIDE DIAMETER (in.): 2.2635
 EFFECTIVE OUTSIDE DIAMETER (in.): 2.238
 INSIDE DIAMETER (in.): 2.006
 CROSS-SECTIONAL AREA (in²): 0.7733
 (WITHOUT COATING)

NOMINAL COATING THICKNESS (in.): 0.0128

MAXIMUM STRESS (ksi)	STRESS RATIO, R	MAXIMUM LOAD (kips)	MINIMUM LOAD (kips)	STRESS CYCLES	COMMENTS
150	-0.33	116.0	-38.7	20	AUDIBLE INDICATIONS DURING CYCLE 1.
160	-0.33	123.7	-41.2	20	
170	-0.33	131.5	-43.8	20	AUDIBLE INDICATIONS FOLLOWED BY SPALLING OF THE COATING.
LOADED AT 2 kips TO THE MEAN LOAD.					

SPECIMEN: HYT 5

OUTSIDE DIAMETER (in.): 2.2633
 EFFECTIVE OUTSIDE DIAMETER (in.): 2.239
 INSIDE DIAMETER (in.): 2.0055
 CROSS-SECTIONAL AREA (in²): 0.7784
 (WITHOUT COATING)

NOMINAL COATING THICKNESS (in.): 0.0122

MAXIMUM STRESS (ksi)	STRESS RATIO, R	MAXIMUM LOAD (kips)	MINIMUM LOAD (kips)	STRESS CYCLES	COMMENTS
140	-0.33	109.0	-36.3	20	AUDIBLE INDICATION DURING CYCLE 1.
150	-0.33	116.8	-38.9	20	AUDIBLE INDICATION DURING CYCLE 1.
160	-0.33	124.5	-41.5	20	AUDIBLE INDICATION DURING CYCLE 17.
170	-0.33	132.3	-44.1	20	AUDIBLE INDICATIONS DURING CYCLES 15-18. CIRCUMFERENTIAL CRACK FORMED BETWEEN CYCLES 15 AND 19.
180	-0.33	140.1	-46.7	20	NUMEROUS CIRCUMFERENTIAL CRACKS FORMED DURING CYCLE 1.
LOADED AT 2 kips TO THE MEAN LOAD.					

SPECIMEN: HYT 6

OUTSIDE DIAMETER (in.): 2.2633
 EFFECTIVE OUTSIDE DIAMETER (in.): 2.239
 INSIDE DIAMETER (in.): 2.0085
 CROSS-SECTIONAL AREA (in²): 0.7689
 (WITHOUT COATING)

NOMINAL COATING THICKNESS (in.): 0.0122

MAXIMUM STRESS (ksi)	STRESS RATIO, R	MAXIMUM LOAD (kips)	MINIMUM LOAD (kips)	STRESS CYCLES	COMMENTS
150	-1	115.3	-115.3	20	AUDIBLE INDICATIONS DURING CYCLE 1. SPECIMEN TESTED WITH A TENSION-COMPRESSION LOAD SEQUENCE.
160	-1	123.0	-123.0	20	AUDIBLE INDICATION DURING CYCLE 1. COMPRESSION-TENSION LOAD SEQUENCE APPLIED DURING THE 180-190 kN TEST SEGMENTS.
170	-1	130.7	-130.7	20	AUDIBLE INDICATIONS DURING CYCLES 1 AND 2. UNIFORMLY SPACED CRACKS PRESENT IN THE GAUGE SECTION AFTER TEST SEGMENT.
180	-1	138.4	-138.4	10	TEST CONTINUED.
190	-1	146.1	-146.1	10	TEST CONTINUED.

SPECIMEN: HYT 7OUTSIDE DIAMETER (in.): 2.2642EFFECTIVE OUTSIDE DIAMETER (in.): 2.240INSIDE DIAMETER (in.): 2.0055CROSS-SECTIONAL AREA (in²): 0.7819
(WITHOUT COATING)NOMINAL COATING THICKNESS (in.): 0.0121

MAXIMUM STRESS (ksi)	STRESS RATIO, R	MAXIMUM LOAD (kips)	MINIMUM LOAD (kips)	STRESS CYCLES	COMMENTS
150	-0.33	117.3	-39.1	20	AUDIBLE INDICATION DURING CYCLE 1.
160	-0.33	125.1	-41.7	20	AUDIBLE INDICATION DURING CYCLE 1. FINE CRACKS ALONG ENTIRE GAUGE LENGTH AT THE END OF THE TEST SEGMENT.
170	-0.33	132.9	-44.3	20	AUDIBLE INDICATION DURING CYCLE 1.
LOADED AT 2 kips/s TO THE MEAN LOAD.					

THIS PAGE INTENTIONALLY LEFT BLANK

DISTRIBUTION:

NAVAIRSYSCOM (AIR-4.3.4, AIR-6.3, AIR-3.2E, AIR-1.1E), Bldg. 2188 48066 Shaw Road, Patuxent River, MD 20670	(25)
NAVAIRSYSCOM (AIR-4.3.3), Bldg. 2187 48110 Shaw Road, Patuxent River, MD 20670	(5)
NAVAVNDEPOT (AIR-6.3, AIR-4.3.4, AIR-4.3.3) NAS North Island, San Diego, CA 92135	(2)
NAVAVNDEPOT (AIR-6.3, AIR-4.3.4, AIR-4.3.3) PSD, Box 8021, Cherry Point, NC 28533-0021	(2)
NAVAVNDEPOT (AIR-6.3, AIR-4.3.4, AIR-4.3.3) NAS Jacksonville, FL 32212	(2)
NAVAIRSYSCOM (PMA-265), Bldg. 2272, Suite 445 47123 Buse Road, Patuxent River, MD 20670-1547	(1)
Joint Strike Fighter Program Office 1213 Jefferson Davis Highway, Suite 600, Arlington, VA 22202-3402	(1)
NAVAIRSYSCOM (AIR-5.1V), Bldg. 304, Room 120 22541 Millstone Road, Patuxent River, MD 20670-1606	(1)
NAVAIRSYSCOM (AIR-5.1), Bldg. 304, Room 100 22541 Millstone Road, Patuxent River, MD 20670-1606	(1)
NAVAIRWARCENACDIV (7.2.5.1), Bldg. 405, Room 108 22133 Arnold Circle, Patuxent River, MD 20670-1551	(1)
NAVTESTWINGLANT (55TW01A), Bldg. 304, Room 200 22541 Millstone Road, Patuxent River, MD 20670-1606	(1)
DTIC 8725 John J. Kingman Road, Suite 0944, Ft. Belvoir, VA 22060-6218	(1)

UNCLASSIFIED

UNCLASSIFIED